Exponential Adams Bashforth ODE solver for stiff problems

Yves Coudière, Charlie Douanla Lontsi, Charles Pierre

Exponential Adams Bashforth ODE solver for stiff problems

Y. COUDIÈRE, C. DOUANLA LONTSI, AND C. PIERRE

Abstract. We analyze in this paper a class of explicit exponential methods for the time integration of stiff differential problems. Precisely, we considered Adams exponential integrators with general varying stabilizers. General stabilization brings flexibility and computational facilities for ODE systems and for semilinear evolution PDEs coupled with ODE systems.
Stability and convergence are proven, by introducing a new framework that extends multistep linear methods. Dahlquist stability is numerically investigated. $A(\alpha)$-stability is observed under a condition on the stabilizer, which is a singular property for explicit schemes. The methods are numerically studied for two stiff models in electrophysiology. Its performances are compared with several classical methods. We conclude that for stiff ODE systems, it provides a cheaper way to compute accurate solutions at large time steps than implicit solvers.

1. Introduction

Stiff differential problems are commonly encountered in many fields and very diverse applications. Stiffness is the source of considerable increase in computational effort. Consider a stiff ODE system, written as a general Cauchy problem,

$$\frac{dy}{dt} = f(t, y), \quad y(0) = y_0. \tag{1}$$

Implicit and explicit methods are classical choices for its resolution. On one hand, implicit methods require non linear solvers that may cause significant additional costs both computationally and in terms of implementation effort for complex applications. On the other hand explicit methods induce the resort to very fine discretization grids in order to maintain stability.

An alternative way is *exponential integrators*: a class of explicit methods meanwhile exhibiting strong stability properties. Exponential integrators motivated many studies along the past 15 years, among which we quote *e.g.* [13, 7, 14, 17, 30, 21] and refer to [23, 15, 12] for general reviews. Numerical instabilities are caused by the eigenvalues of largest negative real part in the system (1) Jacobian

Date: November the 8^{th}, 2016.
2010 *Mathematics Subject Classification.* 65L04, 65L06, 65L20, 65L99.
Key words and phrases. stiff equations, explicit high-order multistep methods, exponential integrators of Adams type, stability and convergence, Dahlquist stability .
This work was supported by the ANR, INRIA and the CNRS.

matrix. The basic idea for exponential integrators is to split equation (1) into a linear part and a non linear part,

$$\frac{dy}{dt} = a(t,y)y + b(t,y), \quad y(0) = y_0. \tag{2}$$

The linear part $a(t,y)$ is used to stabilize the resolution. The stabilization is based on the observation that an exact integration of problem (2) is available when $b(t,y) = 0$ and $a(t,y) = \alpha$ is a constant, by computing $\mathrm{e}^{\alpha h}$ with h the time step. This exponential computation is the additional cost of exponential methods when compared to classical explicit methods.

Exponential integrators of Adams type are explicit multistep methods first introduced in [24, 5] considering a constant linear part $A = a(t,y)$ in (2). The schemes are derived using a multistep polynomial interpolation of Adams Bashforth type in the variation of constants formula. This approach is well suited for semilinear evolution PDEs and their spatial discretization. It recently received an increasing interest [29, 4, 25] and various convergence analysis have been done in this framework [16, 1, 19].

Extensions towards non constant linear parts first have been led in the 70's in [20, 6]. Problem (1) is rewritten as,

$$\frac{dy}{dt} = \alpha_n y + c_n(t,y), \quad y(0) = y_0 \in \mathbb{R}^N,$$

with $\alpha_n y + c_n(t,y) = f(t,y)$ and where α_n, referred to as the *stabilizer*, is updated after each time step. In particular, the *linearized exponential Adams method*, where the stabilizer α_n is set to $\partial_y f(t_n, y_n)$, has been carefully analyzed in [16, 1, 19], where convergence is proven.

However, setting the stabilizer α_n to the Jacobian matrix $\partial_y f(t_n, y_n)$ has several drawbacks. Considering the differential system (1), only part of its equations may need stabilization. In this case, we would like to use only a part of the Jacobian matrix to avoid dispensable computations. Exponential integrators basically require to compute terms of the form $\mathrm{e}^{\alpha_n h}\,\gamma$. In case of an ODE system, this is a matrix vector product, with matrix the exponential of $\alpha_n h$. Its computation is not straightforward, various numerical strategy have been considered so far, see [15, 12] for reviews. This difficulty vanishes when α_n is a diagonal matrix. Nørsett already observed this in its original paper [24]. He actually suggested to use the diagonal part of the Jacobian matrix only. Considering general stabilizers α_n brings a lot of flexibility. More details are given in section 2.4.

We present in this paper a theoretical and numerical analysis for general varying stabilizers α_n. That case will be referred to as *exponential Adams Bashforth* and shortly denoted EAB. Together with the EAB scheme, we introduce a new variant of it, that we called *integral exponential Adams Bashforth*, denoted I-EAB. Convergence and stability results will be proven for these two methods.

A general explicit *linear multistep method* (see *e.g.* [10]) formulates as,

$$y_{n+1} = M(h)Y + h\Psi_h(t_n, Y),$$

where $Y = (y_n, \ldots, y_{n-k+1})$ is a vector composed of the k data at time instant $t_n, \ldots, t_{n-k+1}$. It involves a constant linear part $M(h)$ and a non linear Lipschitz function Ψ_h. For such methods, a classical result stares that (see *e.g.* [10, chapter III.4]) convergence is equivalent to consistency and stability under perturbation. However, for EAB methods, the linear part above depends on the stabilizer α_n. It is of the form $M(h, \alpha_n)$ and is no longer constant. Hence, EAB methods are not linear multistep method. The previous theorem of convergence does not apply and an alternative analysis is needed.
We develop here an extension of this theorem towards multistep exponential integrators. General sufficient conditions for stability under perturbation and convergence are given in theorem 1. Then this theorem is used to prove convergence and stability under perturbation for the EAB and I-EAB schemes with varying stabilizer α_n

Consider the linear equation $y' = \lambda y$. When setting the stabilizer as $\alpha_n = \lambda$, exponential integrators are exact and so A-stable. However, when considering general stabilizers, the relationship between the Dahlquist stability and the stabilizer definition has to be studied. We analyze the *Dahlquist stability* properties of EAB methods with that point of view in this paper. Following a concept introduced in [26], the Dahlquist stability domain is defined up to a parameter θ. This parameter measures with what accuracy the stabilizer α_n approximates the system Jacobian matrix.
We numerically establish that EAB methods are $A(\alpha)$ stable provided that the stabilizer is sufficiently close to the system Jacobian matrix (precise definitions are in section 5). Moreover the angle α approaches $\pi/2$ when the stabilizer goes to the system Jacobian matrix. In contrast, there exists no $A(0)$ stable explicit linear multistep method (see [11, chapter V.2]). This property is quite remarkable for explicit methods.

We provide a numerical analysis for the EAB and I-EAB scheme properties, including comparisons with several classical methods. We considered for this an application in *cardiac electrophysiology*. Models in cardiac electrophysiology display stiff behaviors. Exponential integrators have already been studied for their resolution in [26, 3]. We here set the stabilizer to a part of the Jacobian matrix diagonal, that corresponds to the model stiffest equations. Robustness to stiffness is studied with this choice. It is numerically shown to be comparable as for implicit methods both in terms of accuracy and of stability condition on the time step. We conclude that EAB methods are well suited for solving stiff differential problems. In particular they allow computations at large time step with good accuracy properties and cheap cost.

The paper is organized as follows. The EAB and I-EAB methods are introduced in section 2. In section 3 is stated and demonstrated the general convergence and stability theorem. Convergence and stability under perturbation for EAB and I-EAB scheme proofs follow in section 4. In section 5 is investigated the Dahlquist stability properties of EAB method and the numerical experiments end this paper in section 6.

2. Scheme definition

The methods presented here are k-multistep methods with time step h. The numerical solution y_{n+1} at time instant $t_{n+1} = (n+1)h$ is computed using the numerical data $y_n, \dots, y_{n-k+1}$ at time instants $t_n, \dots, t_{n-k+1}$.

2.1. **Recall on Adams Bashforth.** That classical scheme, see e.g. [10], follows from the integration of eq. (1) on (t_n, t_{n+1}),

$$y(t_{n+1}) = y(t_n) + \int_{t_n}^{t_{n+1}} f(\tau, y(\tau))d\tau.$$

The method is defined by replacing in this formula the function $t \mapsto f(t, y(t))$ by its Lagrange polynomial $\tilde{f}_n$ at time steps $t_n \dots t_{n-k+1}$. Precisely $\tilde{f}_n$ is the polynomial of lowest degree satisfying $\tilde{f}_n(t_{n-j}) = f(t_{n-j}, y_{n-j})$ for $j = 0 \dots k-1$. This yields the numerical scheme $y_{n+1} = y_n + \int_{t_n}^{t_{n+1}} \tilde{f}_n(\tau)d\tau$.

2.2. **The Integral Exponential Adams Bashforth method of order k.** Shortly denoted I-EAB$_k$, the method applies to problem (2). It is based on the variation of constants formula,

$$y(t_{n+1}) = \mathrm{e}^{g(t_{n+1})} \left(y(t_n) + \int_{t_n}^{t_{n+1}} \mathrm{e}^{-g(\tau)}\, b(y(\tau), \tau)d\tau \right),$$

where $g(t) = \int_{t_n}^{t} a(\tau, y(\tau))d\tau$. The numerical scheme is obtained by replacing the two functions $t \mapsto a(t, y(t))$ and $t \mapsto b(t, y(t))$ by their Lagrange polynomials $\tilde{a}_n$ and $\tilde{b}_n$ at time steps $t_n \dots t_{n-k+1}$. Precisely $\tilde{a}_n$ and $\tilde{b}_n$ are the two polynomials of lowest degree that satisfy $\tilde{a}_n(t_{n-j}) = a(t_{n-j}, y_{n-j})$ and $\tilde{b}_n(t_{n-j}) = b(t_{n-j}, y_{n-j}))$ for $j = 0 \dots k-1$,. The I-EAB$_k$ scheme is given by,

$$y_{n+1} = \mathrm{e}^{\tilde{g}_n(t_{n+1})} \left(y_n + \int_{t_n}^{t_{n+1}} \mathrm{e}^{-\tilde{g}_n(\tau)}\, \tilde{b}_n(\tau)d\tau \right), \tag{3}$$

where $\tilde{g}_n(t) = \int_{t_n}^{t} \tilde{a}_n(\tau)d\tau$.
In practice, a quadrature rule is required to evaluate y_{n+1}, details are given in section 6.2.

2.3. **Case of a constant linear part.** When $a(t,y)=\alpha$ is a constant, y_{n+1} in eq. (3) can be computed explicitly. In this case we have $\tilde{a}_n(t)=\alpha$, $g(t)=\alpha(t-t_n)$ and the interpolation polynomial $\tilde{b}_n(t)$ reads,

$$\tilde{b}_n(t)=\sum_{j=0}^{k-1}\frac{\beta_{nj}}{j!}\left(\frac{t-t_n}{h}\right)^j,$$

where the coefficients $(\beta_{nj})_{j=0\dots k-1}$, given in table 1, are the unique solution to the linear system,

$$\sum_{j=0}^{k-1}\frac{\beta_{nj}}{j!}(-i)^j=b(t^{n-i},y_{n-i}):=b_{n-i},\quad i=0\dots k-1.$$

With these notations, formula (3) becomes,

$$\begin{aligned}y_{n+1}&=\mathrm{e}^{\alpha h}\,y_n+\mathrm{e}^{\alpha h}\sum_{j=0}^{k-1}\int_{t_n}^{t_{n+1}}\mathrm{e}^{-\alpha(s-t_n)}\,\frac{\beta_{nj}}{j!}\left(\frac{s-t_n}{h}\right)^j ds\\&=\mathrm{e}^{\alpha h}\,y_n+h\sum_{j=0}^{k-1}\beta_{nj}\int_0^1\mathrm{e}^{\alpha h(1-\theta)}\,\frac{\theta^j}{j!}d\theta,\end{aligned}$$

and finally,

$$y_{n+1}=\mathrm{e}^{\alpha h}\,y_n+h\sum_{j=0}^{k-1}\varphi_{j+1}(\alpha h)\beta_{nj},\tag{4}$$

where the functions φ_j, originally introduced in [24], are defined by by the recursive relations,

$$\varphi_0(z)=\mathrm{e}^z,\quad \varphi_{j+1}(z)=\frac{\varphi_j(z)-\varphi_j(0)}{z}\quad\text{and}\quad\varphi_j(0)=\frac{1}{j!}.\tag{5}$$

TABLE 1. Coefficients β_{nj} for the I-EAB$_k$ schemes, case $a(t,y)=\alpha$ – and for the EAB$_k$ schemes (read c instead of b).

k	1	2	3	4
β_{n0}	b_n	b_n	b_n	b_n
β_{n1}	–	b_n-b_{n-1}	$\frac{3}{2}b_n-2b_{n-1}+\frac{1}{2}b_{n-2}$	$\frac{11}{6}b_n-3b_{n-1}+\frac{3}{2}b_{n-2}-\frac{1}{3}b_{n-3}$
β_{n2}	–	–	$b_n-2b_{n-1}+b_{n-2}$	$2b_n-5b_{n-1}+4b_{n-2}-b_{n-3}$
β_{n3}	–	–	–	$b_n-3b_{n-1}+3b_{n-2}-b_{n-3}$

2.4. **The Exponential Adams Bashforth method.** The simplification of the I-EAB$_k$ scheme in case of a constant linear part is very interesting for practical implementation purposes. To benefit from these simplifications with a varying function $a(t,y)$, assume that a constant approximation α_n of $a(t,y)$ on the interval (t_n, t_{n+1}) is available. The coefficient α_n will be called the *stabilizer* at time t_n. Hence equation (2) can be rewritten on each interval (t_n, t_{n+1}) as,

$$\frac{dy}{dt} = \alpha_n y + c_n(t,y) \quad \text{with} \quad c_n(t,y) = b(t,y) + (a(t,y) - \alpha_n)y.$$

As previously, we denote by $\tilde{c}_n$ the Lagrange polynomial of degree at most $k-1$ of the c_n, defined by $\tilde{c}_n(t_{n-i}) = c_n(t_{n-j}, y_{n-i}) := c_{n-i}$ for $i = 0 \dots k-1$. In this framework equation (4) becomes,

$$y_{n+1} = \mathrm{e}^{\alpha_n h}\, y_n + h \sum_{j=0}^{k-1} \varphi_{j+1}(\alpha_n h)\gamma_{nj}, \tag{6}$$

where α_n, γ_{nj} replace α, β_{nj}, and where the functions φ_j are unchanged. The coefficients γ_{nj} can be computed as in table 1 with c_{n-i} instead of b_{n-i}.

Equation (6) defines the *Exponential Adams Bashforth* method of order k, denoted by EAB$_k$. The EAB$_k$ method is characterized by the choice of α_n at the successive time steps. We make the assumption that the stabilizer is defined from the knowledge of the approximation of the k previous time steps,

$$\alpha_n = \alpha(Y, t_n, h), \quad Y = (y_n, \dots, y_{n-k+1}), \quad \alpha \quad \text{continuous.} \tag{7}$$

This definition will naturally depend on $a(t,y)$. For instance, the particular choice $\alpha_n = a(t_n, y_n)$ will be made in the numerical section 6. More general definitions can however be considered: only the following constraint is imposed,

$$\text{if} \quad a(t,y) \quad \text{has a compact support then} \quad |\alpha(Y, t_n, h)| \leq C, \tag{8}$$

with C only depending on the function $(t,y) \to a(t,y)$.

A versatile choice for α_n has significant practical consequences. In particular it makes EAB$_k$ method quite relevant in the context of ODE systems and of reaction diffusion PDEs coupled with ODE systems.

- In the case of an ODE system, α_n is a matrix. The definition of $\varphi_j(\alpha_n h)$ still makes sense since the functions φ_j are analytic (it also makes sense if α_n is a bounded operator on a Banach space). Then, $\varphi_j(\alpha_n h)\gamma$ in eq. (6) is a matrix vector product. Its computation is delicate in general. This has led to various strategy, such as Pade approximations, as developed in [15]. However this difficulty vanishes if α_n is a diagonal matrix. This case is achieved by setting α_n to the Jacobian matrix diagonal.
- Still in case of an ODE system, only part of it might require stabilization. This is realized by setting a block diagonal α_n, as in section 6.

– If α is a negative self adjoint operator, $\varphi_j(\alpha_n h)$ is a bounded operator, since φ_j is bounded on the half complex plane $\{z \in \mathbb{C},\ \mathrm{Re}\ z < 0\}$. This is particularly interesting for reaction diffusion PDEs.
– In case of a reaction diffusion PDE coupled with an ODE system, choosing a block diagonal α_n, with one block related to the diffusion operator, allows to split the PDE / ODE coupling for the computation of $\varphi_j(\alpha_n h)\gamma$.

Let us end with several remarks on the EAB_k method.

– Convergence and stability results for the EAB_k method in section 4 only require conditions (7) and (8) so that α_n can apparently be chosen arbitrarily. However this choice of course impacts the accuracy. The question of the relationship between accuracy and the stabilizer definition will not be studied in this paper.
– The computation of y_{n+1} in eq. (6) requires the computation of $\varphi_j(\alpha_n h)$ for $j = 0, \ldots, k$. This computational effort can be reduced with the recursive definition (5). In practice only $\varphi_k(\alpha_n h)$ needs to be computed. This is detailed in section 6.2.

3. Abstract theory

As developed in section 1, EAB and I-EAB methods do not belong to the linear multistep method class. An alternative formalism is needed for their analysis. It is developed here.

3.1. **Definitions.** Problem (2) is considered on some vector space E equipped with a norm $|\cdot|_E$. We assume that it has a unique solution $y : [0, T] \to E$ for some final time $T > 0$. For a given time step $h < T$, we define the time instants $t_n = nh$ for $0 \le n \le N_h := [T/h]$.
A k-multistep method is given by a scheme generator $S_{h,n}$ that is a mapping defined for all $0 < h < T$, $k - 1 \le n < N_h$ and $Y \in E^k$ by,

$$S_{h,n} : Y = (y_k, \ldots, y_1) \in E^k \mapsto S_{h,n}(Y) = (s_{h,n}(Y), y_k, \ldots, y_2) \in E^k, \tag{9}$$

where $y_{k+1} := s_{h,n}(Y) \in E$ is computed, for instance, from formulas (3) or (6).
A numerical solution is a sequence (Y_n) in E^k for $n = k - 1 \ldots N_h$, so that,

$$Y_{n+1} = S_{h,n}(Y_n), \quad n = k - 1 \ldots N_h - 1.$$

Numerical solutions will be asked to verify the following upper bound on their initial data,

$$|Y_{k-1}|_\infty \le M, \tag{10}$$

where M is a fixed positive constant, and with $|\cdot|_\infty$ the maximum norm on E^k.

A perturbation of a numerical solution (Y_n) is a sequence (Z_n) in E^k for $n = k - 1 \ldots N_h$, so that,

$$Z_{k-1} = Y_{k-1} + \xi_{k-1}, \quad Z_{n+1} = S_{h,n}(Z_n) + \xi_{n+1}, \quad n = k - 1 \ldots N_h - 1,$$

with $\xi_n \in E^k$. We say that the scheme (9) is *stable under perturbation* if there exist constants $C > 0$, $\varepsilon_0 > 0$, and $h_0 > 0$ such that, for all $0 < \varepsilon \leq \varepsilon_0$, for any numerical solution (Y_n) constructed with a time step $h < h_0$ and for all associated perturbation (Z_n) satisfying,

$$|\xi_{k-1}|_\infty \leq \varepsilon \quad \text{and} \quad \max_{n=k\dots N_h} |\xi_n|_\infty \leq h\varepsilon,$$

then we have,

$$\max_{n=k\dots N_h} |Z_n - Y_n|_\infty < C\varepsilon.$$

We denote $Y(t_n) = (y(t_n), \dots, y(t_{n-k+1})) \in E^k$ the k successive values of the exact solution up to the time instant t_n. We say that the scheme (9) is *consistent of order p* if there exist constants $C > 0$ and $h_0 > 0$ such that, for all $0 < h \leq h_0$,

$$\max_{n=k-1\dots N_h-1} |Y(t_{n+1}) - S_{h,n}(Y(t_n))|_\infty \leq Ch^{p+1}.$$

We say that the scheme (9) is *convergent of order p* if there exist constants $C > 0$, and $h_0 > 0$ such that,

$$\max_{n=k\dots N_h} |Y(t_n) - Y_n|_\infty \leq C\left(h^p + |Y(t_{k-1}) - Y_{k-1}|_\infty\right),$$

for all numerical solutions (Y_n) associated with a time step $h < h_0$.

3.2. **Main result.**

Theorem 1 (Convergence)**.** *Suppose that there exist constants $C > 0$ and $h_0 > 0$ such that, for all $0 < h < h_0$, for all $n = k-1 \dots N_h - 1$, and for any $Y, Z \in E^k$,*

$$1 + |S_{h,n}(Y)|_\infty \leq (1 + |Y|_\infty)(1 + Ch), \tag{11}$$

$$|S_{h,n}(Y) - S_{h,n}(Z)|_\infty \leq |Y - Z|_\infty (1 + Ch(1 + |Y|_\infty)); \tag{12}$$

then the scheme is stable under perturbation.
Moreover assume that it is consistent of order p, then it is convergent of order p.

Proof. Consider $C > 0$ and $h_0 > 0$ such that conditions (11) and (12) hold. We set $0 < h < h_0$ and consider a numerical solution (Y_n) for this time step. A recursion on condition (11) gives,

$$1 + |Y_n|_\infty \leq (1 + |Y_{k-1}|_\infty)(1 + Ch)^{n-k+1} \leq \mathrm{e}^{CT}(1 + |Y_{k-1}|_\infty), \tag{13}$$

since $(1 + x)^p \leq \mathrm{e}^{px}$ and $(n - k + 1) \leq T/h$.
Now, consider a perturbation (Z_n) of (Y_n). Using eqs. (12) and (13), we have,

$$\begin{aligned}
|Y_{n+1} - Z_{n+1}|_\infty &\leq |S_{h,n}(Y_n) - S_{h,n}(Z_n)|_\infty + |\xi_{n+1}|_\infty \\
&\leq |Y_n - Z_n|_\infty (1 + Ch(1 + |Y_n|_\infty)) + |\xi_{n+1}|_\infty \\
&\leq |Y_n - Z_n|_\infty \left(1 + Ch\,\mathrm{e}^{CT}(1 + |Y_{k-1}|_\infty)\right) + |\xi_{n+1}|_\infty \\
&\leq |Y_n - Z_n|_\infty (1 + C^\star h) + |\xi_{n+1}|_\infty,
\end{aligned}$$

where $C^\star := C\,\mathrm{e}^{CT}\,(1+M)$ and with M in eq. (10).
By recursion on n, we get for $n = k, \dots N_h$,

$$|Y_n - Z_n|_\infty \le (1+C^\star h)^{n-k+1}\,|Y_{k-1} - Z_{k-1}|_\infty + \sum_{i=0}^{n-k} (1+C^\star h)^i\,|\xi_{n+1-i}|_\infty$$

$$\le \mathrm{e}^{c^\star T}\,|\xi_{k-1}|_\infty + \max_{j=k\dots n+1} |\xi_j|_\infty \sum_{i=0}^{n-k} (1+C^\star h)^i\,.$$

The geometrical sum can be computed,

$$\sum_{i=0}^{n-k} (1+C^\star h)^i = \frac{(1+C^\star h)^{n-k+1}-1}{C^\star h} \le \frac{\mathrm{e}^{C^\star T}-1}{C^\star h} \le \frac{T}{h}\,\mathrm{e}^{C^\star T},$$

because $(\mathrm{e}^x - 1)/x \le \mathrm{e}^x$ for positive x. It follows that,

$$|Y_n - Z_n|_\infty \le \mathrm{e}^{C^\star T}\left(|\xi_{k-1}|_\infty + T \max_{j=k\dots n+1} |\xi_j|_\infty/h\right),$$

and the scheme is stable under perturbation.

Now assume that the scheme is also consistent of order p. We also denote by C the consistency constant. Splitting the total error between consistency and perturbation errors gives:

$$\begin{aligned}
|Y(t_{n+1}) - Y_{n+1}|_\infty &= |Y(t_{n+1}) - S_{h,n}(Y_n)|_\infty \\
&\le |Y(t_{n+1}) - S_{h,n}(Y(t_n))|_\infty + |S_{h,n}(Y(t_n)) - S_{h,n}(Y_n)|_\infty \\
&\le Ch^{p+1} + |Y(t_n) - Y_n|_\infty (1 + Ch(1 + |Y_n|_\infty)) \\
&\le Ch^{p+1} + |Y(t_n) - Y_n|_\infty (1 + C^\star h),
\end{aligned}$$

by using eq. (13) in the last line. With a recursion on n,

$$|Y(t_n) - Y_n|_\infty \le (1+C^\star h)^{n-k+1}\,|Y(t_{k-1}) - Y_{k-1}|_\infty + Ch^{p+1} \sum_{i=0}^{n-k} (1+C^\star h)^i$$

$$\le \mathrm{e}^{c^\star T}\,|Y(t_{k-1}) - Y_{k-1}|_\infty + T\,\mathrm{e}^{c^\star T}\,h^p,$$

using the same upper bounds as previously. This last inequality states convergence of order p and ends the proof. □

4. I-EAB$_k$ and EAB$_k$ stability and convergence

Definitions and notations of section 3 are considered here. We recall that for the EAB$_k$ scheme the stabilizer α_n is given by the general definition (7) assumed to satisfy (8).

Theorem 2. *Assume that the functions a and b in problem (2) are $C^k([0,T]\times\mathbb{R})$. Then the I-EAB$_k$ and EAB$_k$ schemes are stable under perturbation and convergent of order k.*

We proved theorem 2 in the case $E = \mathbb{R}$ only. The proof key arguments are a Gronwall's inequality, polynomial interpolation and the Urysohn's Lemma. These three tools holding for $E = \mathbb{R}^n$, adaptation of theorem 2 in the case of ODE system is above all technical and has not been carried out here for the sake of simplicity. In the case of a reaction diffusion equation, where E is a Hilbert space, extension of the given proof of theorem 2 is more delicate. In particular the Urysohn's Lemma considered here does not apply. This will imply to strengthen the general assumption *'a and b are $C^k([0,T] \times E)$'*, at least by adding *'uniformly Lipschitz in y'*.

Proof. If the functions a and b have C^k regularity, consistency of order k is ensured by the consistency lemma 4. If they moreover have compact support, the stability lemma 5 states that the stability conditions (11) and (12) are satisfied. Therefore the convergence theorem 1 applies and the I-EAB$_k$ and EAB$_k$ schemes are stable under perturbation and convergent of order k.

Now, for general C^k functions a and b, consider $\mathcal{O}$ a bounded open domain of $[0,T] \times \mathbb{R}$ containing the graph of the solution: $\{(t, y(t)),\ t \in [0,T]\} \subset \mathcal{O}$. Using the Urysohn's lemma, we can consider two C^k functions $\tilde{a}$ and $\tilde{b}$ with compact supports so that $a(t,y) = \tilde{a}(t,y)$ and $b(t,y) = \tilde{b}(t,y)$ for $(t,y) \in \mathcal{O}$.
By assumption, the function $y(t)$ also is the solution of the equation $y' = \tilde{a}(t,y)y + \tilde{b}(t,y)$ with $y(0) = y_0$. We have convergence of order k for the I-EAB$_k$ and EAB$_k$ schemes on this problem. Therefore, for sufficiently small time step and sufficiently small distance between the numerical and exact initial data, the numerical solution for this problem is inside $\mathcal{O}$. But then this numerical solution also is a numerical solution for the original problem $y' = a(t,y)y + b(t,y)$ with $y(0) = y_0$. Then, under these conditions we have coincidence of the numerical solutions of these two problems. This implies convergence of order k and stability under perturbation for the original problem. □

4.1. **Preliminary results.** An additional notation for Lagrange interpolation is needed. Let a continuous function $f : (t,y) \in [0,T] \times \mathbb{R} \mapsto f(t,y) \in \mathbb{R}$, $0 < h < T$, $n = k-1 \dots N_h$ and $Y = (y_k, \dots, y_1) \in \mathbb{R}^k$. The Lagrange polynomial $P_{h,n}(f,Y)$ satisfying,

$$P_{h,n}(f,Y)(t_{n-i}) = f(t_{n-i}, y_{k-i}) \quad \text{for} \quad i = 0 \dots k-1,$$

of degree at most $k-1$, is considered.

With this notation, an obvious consequence of formula (3) is the following definition for the I-EAB$_k$ and EAB$_k$ scheme generators.

Lemma 1 (Generator)**.** *Let $0 < h < T$, $n = k-1 \dots N_h$ and $Y = (y_k, \dots, y_1) \in \mathbb{R}^k$. Consider the problem,*

$$\frac{dz}{dt} = P_{h,n}(a,Y)z + P_{h,n}(b,Y), \quad z(t_n) = y_k, \tag{14}$$

then the I-EAB$_k$ scheme generator satisfies $s_{h,n}(Y) = z(t_{n+1})$.

Alternatively consider the problem (recalling that $c_n(t,y) = b(t,y) - (a(t,y) - \alpha_n)y$*),*

$$\frac{dz}{dt} = \alpha_n z + P_{h,n}(c_n, Y), \quad z(t_n) = y_k, \tag{15}$$

then the EAB_k *scheme generator satisfies* $s_{h,n}(Y) = z(t_{n+1})$.

The following Gronwall's inequality (see [9, Lemma 196, p.150]) will be helpful.

Lemma 2 (Gronwall)**.** *Suppose that* $z(t)$ *is a* C^1 *function. If there exist* $\alpha > 0$ *and* $\beta > 0$ *such that* $|z'(t)| \leq \alpha|t| + \beta$ *for all* $t \in [t_0, t_0 + h]$*, then* $|z(t)| \leq |z(t_0)|\,\mathrm{e}^{\alpha h} + \beta h\,\mathrm{e}^{\alpha h}$*, for all* $t \in [t_0, t_0 + h]$.

Eventually, estimates on Lagrange interpolating polynomials are required.

Lemma 3 (Interpolation)**.** *There exists a constant* $C_L > 0$ *such that, for any continuous function* $f : (t,y) \in [0,T] \times \mathbb{R} \mapsto f(t,y) \in \mathbb{R}$*, for all* $0 < h < T$*,* $k - 1 \leq n \leq N_h - 1$*, we have, for all* $Y, Z \in \mathbb{R}^k$*,*

$$\sup_{t \in (t_n, t_{n+1})} |P_{h,n}(f,Y)(t)| \leq C_L \max_{i=0\ldots k-1} |f(t_{n-i}, y_{k-i})|\,,$$

and

$$\sup_{t \in (t_n, t_{n+1})} |P_{h,n}(f,Y)(t) - P_{h,n}(f,Z)(t)| \leq C_L \max_{i=0\ldots k-1} |f(t_{n-i}, y_{k-i}) - f(t_{n-i}, z_{k-i})|\,.$$

In addition, if the function f *is* $C^k([0,T] \times \mathbb{R})$*, then, for all function* $y : [0,T] \to \mathbb{R}$ *of class* C^k*, and with the notation* $Y(t_n) = (y(t_{n-i}))_{i=0\ldots k-1}$*, we have*

$$\sup_{t \in (t_n, t_{n+1})} |f(t, y(t)) - P_{h,n}(f, Y(t_n))(t)| \leq \sup_{[0,T]} \left| \frac{d^k}{dt^k} \left(f(t, y(t)) \right) \right| h^k.$$

Proof. We first define the reference mapping $\mathcal{L} : Y = (y_k \ldots y_1) \in \mathbb{R}^k \mapsto \mathcal{L}_Y$ where $\mathcal{L}_Y$ is the polynomial of degree at most k so that, $\mathcal{L}_Y(-i) = y_{k-i}$ for $i = 0 \ldots k-1$. We have, for any function $f(t,y)$, and any $0 < h < T$, $k - 1 \leq n \leq N_h - 1$,

$$P_{h,n}(f,Y)(t) = \mathcal{L}_F\left(\frac{t - t_n}{h}\right), \quad \text{where } F = (f(t_{n-i}, y_{k-i}))_{i=0\ldots k-1}\,.$$

The space of the polynomial q of degree $k-1$ is supplied with the uniform norm $|q|_\infty = \sup_{0<\xi<1} |q(\xi)|$. With that norm we denote by C_L the norm of the linear mapping $\mathcal{L}$ (that only depends on k). We have,

$$\sup_{t_n < t < t_{n+1}} |P_{h,n}(f,Y)(t)| = \sup_{0<\xi<1} |\mathcal{L}_F(\xi)| \ = |\mathcal{L}_F|_\infty \leq C_L |F|_\infty = C_L \max_{i=0\ldots k-1} |f(t_{n-i}, y_{k-i})|.$$

This proves the first bound of the interpolation lemma 3.
Consider $Z \in \mathbb{R}^k$ and $G = (f(t_{n-i}, z_{k-i}))_{i=0\ldots k-1}$. Since $\mathcal{L}$ is linear, we have

$|P_{h,n}(f,Y)(t) - P_{h,n}(f,Z)(t)| = \left|\mathcal{L}_{F-G}\left(\frac{t-t_n}{h}\right)\right|$, for all $t \in (t_n, t_{n+1})$. As previously,

$$\sup_{t_n<t<t_{n+1}} |P_{h,n}(f,Y)(t) - P_{h,n}(f,Z)(t)| \leq C_L \max_{i=0\ldots k-1} |f(t_{n-i}, y_{k-i}) - f(t_{n-i}, z_{k-i})|,$$

which proves the second bound of the interpolation lemma 3.
At last, with the assumptions in lemma 3, the function $\phi : t \in [0,T] \mapsto f(t, y(t))$ is of class $C^k([0,T])$. A classical result on Lagrange interpolation applied to ϕ states that, for all $t \in (t_n, t_{n+1})$, there exists $\xi \in (t_{n-k+1}, t_{n+1})$, such that $f(t,y(t)) - \mathcal{L}_F\left(\frac{t-t_n}{h}\right) = \frac{1}{k!}\phi^{(k)}(\xi)\pi(t)$, where $\pi(t) = \prod_{i=0}^{k-1}(t - t_{n-i})$. For $t \in (t_n, t_{n+1})$, we have $|\pi(t)| \leq k!\, h^k$, which proves the last bound of the interpolation lemma 3. □

4.2. **Consistency analysis.**

Lemma 4 (Consistency)**.** *Assume that the functions a and b in problem (2) are $C^k([0,T]\times\mathbb{R})$. Then the I-EAB$_k$ and EAB$_k$ schemes are consistent of order k.*

Proof. Consider the I-EAB$_k$ scheme. With the generator lemma 1, the scheme generator satisfies $s_{h,n}(Y(t_n)) = z(t_{n+1})$ where z is the solution to problem (14). Hence,

$$|(y-z)'| \leq |P_{h,n}(a, Y(t_n))|\,|y-z| + |P_{h,n}(a,Y(t_n)) - a(t,y)|\,|y| + |P_{h,n}(b,Y(t_n)) - b(t,y)|.$$

With the interpolation lemma 3 we get $|(y-z)'| \leq \alpha|y-z| + \beta h^k$, with:

$$\alpha = C_L \sup_{[0,T]} |a(t,y(t))|, \quad \beta = \sup_{[0,T]}|y| \sup_{[0,T]} \left|\frac{d^k}{dt^k} a(t,y(t)\right| + \sup_{[0,T]} \left|\frac{d^k}{dt^k} b(t,y(t))\right|.$$

The constants α and β only depend on the solution y, and the data a, b, T, and k. Finally, we can use the Gronwall's lemma 2 to prove that,

$$|y(t_{n+1}) - s_{h,n}(Y(t_n))| = |y(t_{n+1}) - z(t_{n+1})| \leq |y(t_n) - z(t_n)|\,\mathrm{e}^{\alpha h} + \left(\beta h^k\right) h\,\mathrm{e}^{\alpha h} \leq \beta\,\mathrm{e}^{\alpha T}\, h^{k+1},$$

because $z(t_n) = y(t_n)$. This proves the consistency for the I-EAB$_k$ scheme.

For the EAB$_k$ scheme, $s_{h,n}(Y(t_n)) = z(t_{n+1})$ where z is the solution to problem (15). It follows that,

$$|(y-z)'| \leq |\alpha_n||y-z| + |P_{h,n}(c_n, Y(t_n)) - c_n(t,y)|.$$

With definition (7), the stabilizer can be uniformally bounded, $\alpha_n \leq \alpha$ on the solution y graph for $0 \leq t \leq T$ and for $0 \leq h \leq h_0$. Similarly, the functions $c_n(t,y(t)) = b(t,y(t)) + (a(t,y(t)) - \alpha_n)y(t)$ have uniformly bounded k^{th} derivative on $[0,T]$. Proceeding as previously, we get the consistency for the EAB$_k$ scheme. □

4.3. **Stability analysis.**

Lemma 5 (Stability)**.** *Assume that the functions a and b in problem* (2) *are $C^k([0,T]\times\mathbb{R})$ with compact support. Then the I-EAB$_k$ and EAB$_k$ schemes are stable under perturbations.*
More precisely, the stability conditions (11) *and* (12) *in the convergence theorem 1 are satisfied by the I-EAB$_k$ and EAB$_k$ schemes.*

Proof. Let us first consider the I-EAB$_k$ scheme. By assumption on a and b , we can choose a constant $C>0$ such that,

$$C_L \sup_{[0,T]\times R}|a(t,y)|\le C,\quad C_L \sup_{[0,T]\times R}|\partial_y a(t,y)|\le C,$$
$$C_L \sup_{[0,T]\times R}|b(t,y)|\le C,\quad C_L \sup_{[0,T]\times R}|\partial_y b(t,y)|\le C.$$

With the interpolation lemma 3, we also have for all Y and $Z\in\mathbb{R}^k$, and all $t\in(t_n,t_{n+1})$,

$$|P_{h,n}(a,Y)(t)|\le C,\quad |P_{h,n}(a,Y)(t)-P_{h,n}(a,Z)(t)|\le C|Y-Z|_\infty,$$
$$|P_{h,n}(b,Y)(t)|\le C,\quad |P_{h,n}(b,Y)(t)-P_{h,n}(b,Z)(t)|\le C|Y-Z|_\infty.$$

For $Y\in\mathbb{R}^k$ consider y the solution of equation (14). For all $t\in(t_n,t_{n+1})$ we have $|y'|\le C(|y|+1)$. The Gronwall's lemma 2 gives $|y(t)|\le \mathrm{e}^{Ch}(|y_k|+Ch)$ on (t_n,t_{n+1}). With the generator lemma 1 we have $s_{h,n}(Y)=y(t_{n+1})$. We get from this,

$$|s_{h,n}(Y)|\le |Y|_\infty \mathrm{e}^{Ch}+Ch\,\mathrm{e}^{Ch}\le |Y|_\infty(1+Ch\,\mathrm{e}^{Ch})+Ch\,\mathrm{e}^{Ch},$$

since $\mathrm{e}^x\le 1+x\,\mathrm{e}^x$ for $x=Ch$ and $|y_k|\le|Y_\infty|$. Then,

$$1+|s_{h,n}(Y)|\le(1+|Y|_\infty)(1+Ch\,\mathrm{e}^{Ch}).$$

which proves the stability condition (11) because $|S_{h,n}(Y)|_\infty\le\max(|s_{h,n}(Y)|,|Y|_\infty)$. Being given $Y,Z\in\mathbb{R}^k$, and the associated solutions y and z in eq. (14), we have,

$$(y-z)'=(P_{h,n}(a,Y)-P_{h,n}(a,Z))y+P_{h,n}(a,Z)(y-z)+P_{h,n}(b,Y)-P_{h,n}(b,Z).$$

The following bound for $t\in(t_n,t_{n+1})$ follows,

$$\begin{aligned}|(y-z)'|&\le C|y-z|+C|Y-Z|_\infty(|y|+1)\\&\le C|y-z|+C|Y-Z|_\infty\big((|Y|_\infty+Ch)\,\mathrm{e}^{Ch}+1\big)\\&\le C|y-z|+C|Y-Z|_\infty(1+Ch\,\mathrm{e}^{Ch})(1+|Y|_\infty),\end{aligned}$$

where $|y(t)|$ has been substituted by its bound $(|Y|_\infty+Ch)\,\mathrm{e}^{Ch}$. Using the Gronwall's lemma 2 together with the generator lemma 1 we get,

$$|s_{h,n}(Y)-s_{h,n}(Z)|\le\big(|y_k-z_k|+Ch|Y-Z|_\infty(1+Ch\,\mathrm{e}^{Ch})(1+|Y|_\infty)\big)\,\mathrm{e}^{Ch}.$$

Because $|y_k - z_k| \leq |Y-Z|_\infty$ and $|S_{h,n}(Y) - S_{h,n}(Z)| \leq \max(|s_{h,n}(Y) - s_{h,n}(Z)|, |Y - Z|_\infty)$, we obtain,

$$|S_{h,n}(Y) - S_{h,n}(Z)| \leq |Y - Z|_\infty \left(1 + Ch(1 + Ch\,\mathrm{e}^{Ch})(1 + |Y|_\infty)\right) \mathrm{e}^{Ch}.$$

Using again $\mathrm{e}^x \leq 1 + x\,\mathrm{e}^x$ for $x = Ch$ shows that,

$$\left(1 + Ch(1 + Ch\,\mathrm{e}^{Ch})(1 + |Y|_\infty)\right) \mathrm{e}^{Ch} \leq 1 + Ch\,\mathrm{e}^{Ch}\left(2 + Ch\,\mathrm{e}^{Ch}\right)(1 + |Y|_\infty).$$

This proves the stability condition (12).

Let us now consider the EAB_k scheme. The definition $c_n = b + (a - \alpha_n)y$ gives $\partial_y c_n = \partial_y b + y\partial_y a - \alpha_n$. By assumption on a and b and using the condition (8) on α_n, a constant $C > 0$ can be chosen so that,

$$|\alpha_n| \leq C, \quad C_L \sup_{[0,T]\times R} |c_n(t,y)| \leq C(1 + |y|), \quad \sup_{[0,T]\times R} |\partial_y c_n(t,y)| \leq C(1 + |y|).$$

The interpolation lemma 3 then ensures that,

$$\begin{aligned} &|P_{h,n}(c_n, Y)(t)| \leq C(1 + |Y|_\infty), \\ &|P_{h,n}(c_n, Y)(t) - P_{h,n}(c_n, Z)(t)| \leq C(1 + |Y|_\infty)|Y - Z|_\infty. \end{aligned}$$

For $Y \in \mathbb{R}^k$ consider y the solution of equation (15). For all $t \in (t_n, t_{n+1})$ we have $|y'| \leq C|y| + C(1 + |Y|_\infty)$. The Gronwall's lemma 2 gives $|y(t_{n+1})| \leq (|Y|_\infty + Ch(1 + |Y|_\infty))\,\mathrm{e}^{Ch}$. With the generator lemma 1, $y(t_{n+1}) = s_{h,n}(Y)$. We get,

$$\begin{aligned} 1 + |s_{h,n}(Y)| &\leq 1 + |Y|_\infty(1 + Ch\,\mathrm{e}^{Ch}) + Ch\,\mathrm{e}^{Ch}(1 + |Y|_\infty) \\ &\leq (1 + |Y|_\infty)(1 + 2Ch\,\mathrm{e}^{Ch}), \end{aligned}$$

with the inequality $\mathrm{e}^x \leq 1 + x\,\mathrm{e}^x$ for $x = Ch$. This proves the stability condition (10) because $|S_{h,n}(Y)|_\infty \leq \max(|s_{h,n}(Y)|, |Y|_\infty)$.
Consider now $Z \in \mathbb{R}^k$ and the associated solutions z of equation (15) so that $z(t_{n+1}) = s_{h,n}(Z)$. We have,

$$|y' - z'| \leq C|y - z| + C(1 + |Y|_\infty)|Y - Z|_\infty.$$

The Gronwall's inequality yields,

$$\begin{aligned} |S_{h,n}(Y) - S_{h,n}(Z)| &\leq |Y - Z|_\infty \left(1 + Ch(1 + |Y|_\infty)\right) \mathrm{e}^{Ch} \\ &\leq |Y - Z|_\infty \left(1 + Ch\,\mathrm{e}^{Ch} + Ch\,\mathrm{e}^{Ch}(1 + |Y|_\infty)\right) \\ &\leq |Y - Z|_\infty \left(1 + 2Ch\,\mathrm{e}^{Ch}(1 + |Y|_\infty)\right), \end{aligned}$$

that proves condition (12) for the EAB_k scheme and ends this proof. □

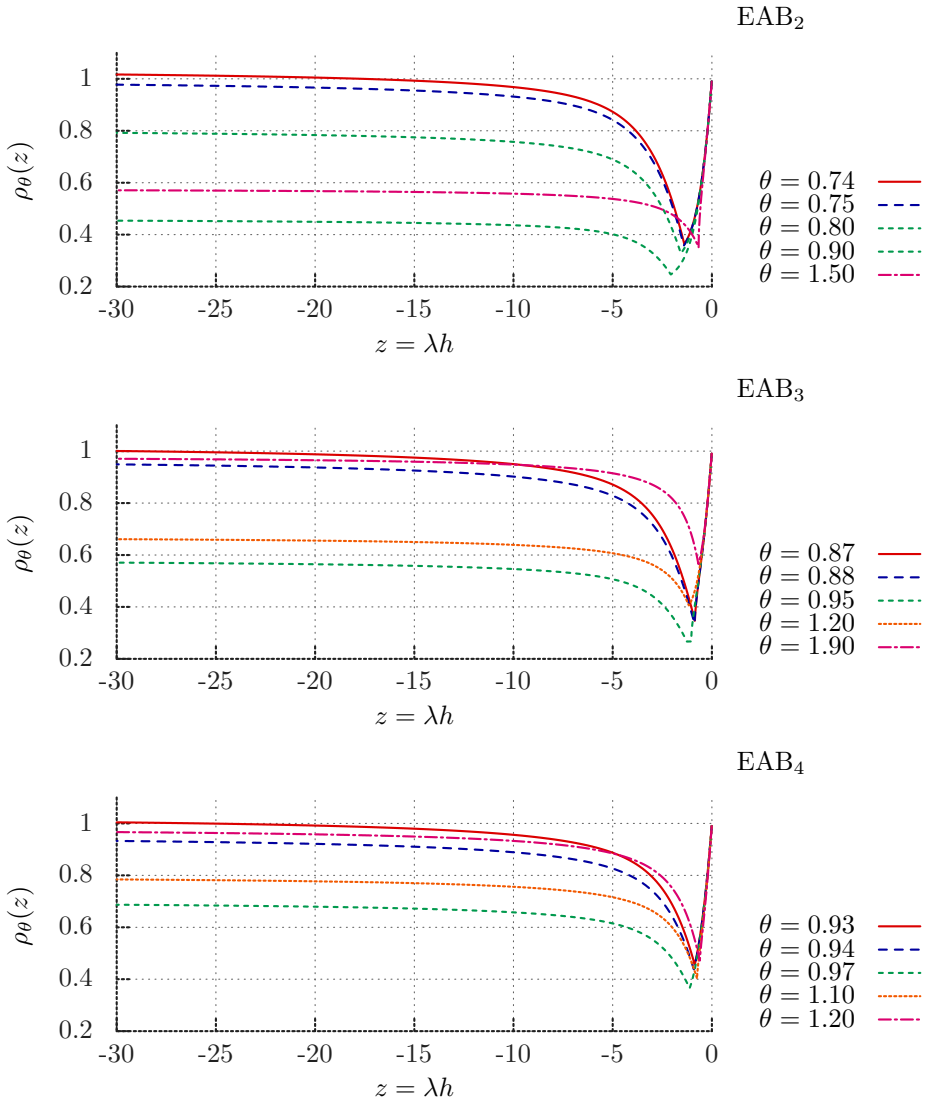

FIGURE 1. On the three figures the function $z \in \mathbb{R}^- \mapsto \rho_\theta(z)$ have been plotted for various values of θ. $A(0)$ stability holds when $\lim_{-\infty} \rho_\theta(z) < 1$.

5. Dahlquist stability

We consider in this section the problem (1) for the *Dahlquist test function* $f(t, y) = \lambda y$. For $\mathrm{Re}(\lambda) < 0$, the exact solution satisfies $|y(t_{n+1})/y(t_n))| = \rho < 1$. Numerical solutions for linear multistep methods satisfy, see e.g. [11],

$$\left| \frac{y_{n+1}}{y_n} \right| \leq \rho(\lambda h),$$

where the function $\rho : \mathbb{C} \to \mathbb{R}^+$ is defined pointwise by the maximum root modulus of a family of polynomial depending on $z = \lambda h$. The stability domain is defined by $D = \{z \in \mathbb{C}, \quad \rho(z) < 1\}$. The scheme is said to be:

- A stable if $\mathbb{C}^- \subset D$,
- $A(\alpha)$ stable if D contains the cone with axis $\mathbb{R}^-$ and with half angle α,
- $A(0)$ stable if $\mathbb{R}^- \subset D$,
- stiff stable if D contains a half plane Re $z < x \in \mathbb{R}^-$.

Let us note that the I-EAB$_k$ and EAB$_k$ schemes coincide when considering the Dahlquist test functions, which have a constant linear part. In the case $\alpha_n = \lambda$, the scheme is exact, and thus A stable. However, when considering general stabilizer α_n, this equality does not hold. The following splitting is introduced,

$$f(t, y) = \lambda y = a(t, y)y + b(t, y), \quad a(t, y) = \theta\lambda \quad \text{and} \quad b(t, y) = \lambda(1 - \theta)y,$$

The parameter $\theta > 0$ controls with what accuracy the exact linear part of $f(t, y)$ in eq. (1) is approximated by $a(t, y)$ in eq. (2). Ideally, we would have $\theta = 1$, but practically, $\theta \neq 1$, though we may hope that $\theta - 1$ is small.
In the framework of exponential methods, the Dahlquist stability domain is defined as D_θ, depending on the parameter θ, and associated to the stability function $\rho_\theta(z)$. This concept had already been introduced in a similar way in [26].

5.1. $A(0)$ **stability.** The stability functions $\rho_\theta(z)$ are numerically studied for $z \in \mathbb{R}^-$. These functions have been plotted for different values of the parameter θ. The results are depicted on fig. 1. In all cases, we conjecture the existence of a limit as $z \to -\infty$. The scheme is $A(0)$ stable when this limit is lower than 1. From Figure 1,

- EAB$_2$ scheme is $A(0)$ stable if $\theta \geq 0.75$,
- EAB$_3$ scheme is $A(0)$ stable if $0.88 \leq \theta \leq 1.9$,
- EAB$_4$ scheme is $A(0)$ stable if $0.94 \leq \theta \leq 1.2$.

Roughly speaking, $A(0)$ stability holds for the EAB$_k$ scheme if the exact linear part of $f(t, y)$ in problem (1) is approximated with an accuracy of 75 %, 85 % or 95% for $k = 2$, 3 or 4 respectively.

5.2. $A(\alpha)$ **stability.** The stability domains D_θ have been plotted for various values of θ taken from fig. 1. The results are depicted on figs. 2 to 4 for $k = 2$ to 4 respectively. Each figure shows the isolines $\rho_\theta(z) = 1$. The stability domain D_θ is on the left of these curves.

- Figure 2 shows that the EAB$_2$ scheme is $A(\alpha)$ stable when $\theta = 0.75$, 0.8 and 0.9 with $\alpha \simeq 50$, 60 and 80 angle degrees respectively.
- Figure 3 displays $A(\alpha)$ stability with $\alpha \simeq 60$, 70 and 60 angle degrees for $\theta = 0.88$, 0.9 and 1.9 respectively for the EAB$_3$ scheme.

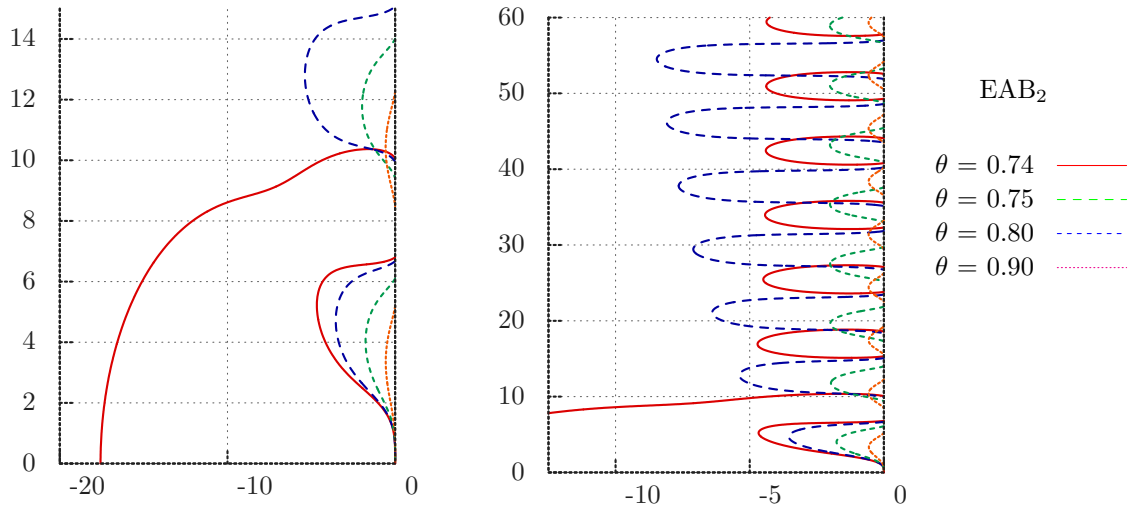

FIGURE 2. Left and right figures show the same isolines $\rho_\theta(z) = 1$ for the EAB_2 scheme, and two ranges of z. The stability domain D_θ is on the left of the isoline.

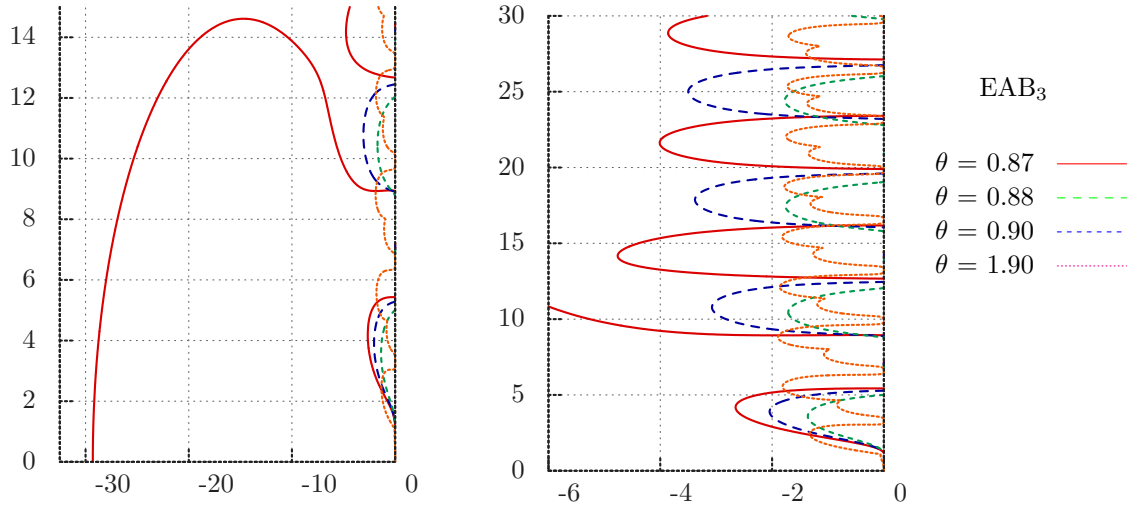

FIGURE 3. Same thing as fig. 2 for the EAB_3 scheme.

- For the EAB_4 scheme eventually, $A(\alpha)$ stability holds with an angle α approximately of 65, 70 and 60 degrees for $\theta = 0.94$, 0.95 and 1.2 respectively, as shown on fig. 4.

In all cases, when $A(\alpha)$ stability is observed, the unstable region inside $\mathbb{C}^-$ is made of a discrete collection of uniformly bounded sets located along the imaginary axes. Hence, the stability domain D_θ also contains half planes of the form $\mathrm{Re}(z) \leq a < 0$.

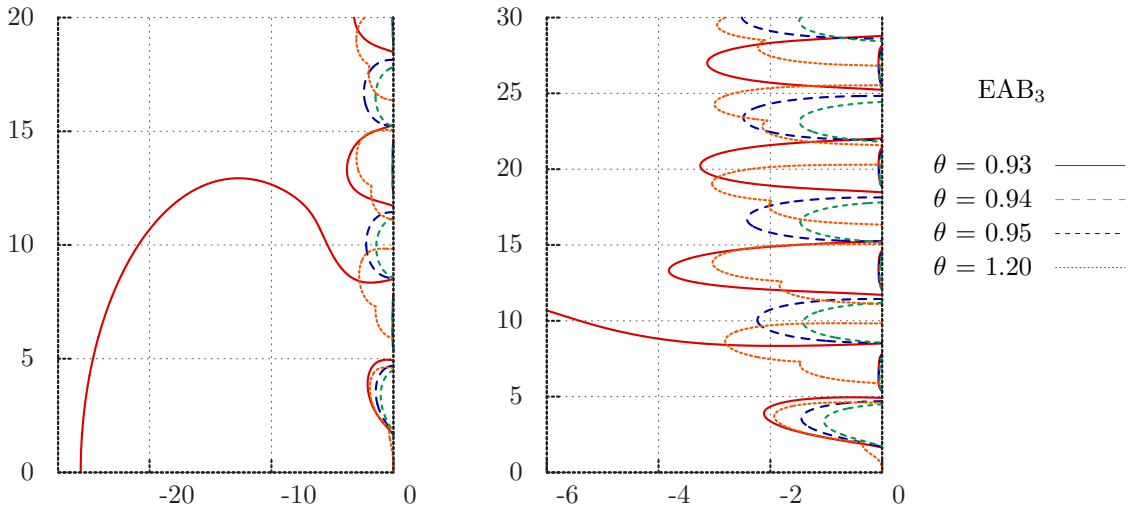

FIGURE 4. Same thing as fig. 2 for the EAB_4 scheme.

We conjecture that, when θ is so that the EAB_k scheme is $A(\alpha)$-stable, then it is also stiff stable.

6. Numerical results

We present in this section numerical experiments that investigate the convergence, accuracy and stability properties of the I-EAB_k and EAB_k schemes.
As an example, they will be applied to a class of stiff models in cardiac electrophysiology. Two models are considered, the Beeler-Reuter model (BR) [2] and the Ten Tusscher *et al.* model (TNNP) [28], both designed for human cardiac cells. The stiffness of these two models is due to the presence of different time scales ranging from 1 ms to 1 s, as depicted on fig. 5. A challenge in this field is to provide accurate and efficient solvers for reaction diffusion PDEs including millions of such cell models (basically one per spatial degree of freedom).
In all this section, for the EAB_k scheme, the stabilizer is defined as $\alpha_n = a(t_n, y_n)$. This definition satisfies the two conditions (7) and (8). For the chosen application, α_n will always be a diagonal matrix.

6.1. Application context.

Classical models used to simulate the electrical activity of cardiac cells are stiff ODE systems of the form, see [18, 2, 22, 28]:

$$\begin{aligned} \frac{dw_i}{dt} &= \frac{w_{\infty,i}(v) - w_i}{\tau_i(v)}, \qquad \frac{dc}{dt} = g(w, c, v), \\ \frac{dv}{dt} &= -I_{\mathrm{ion}}(w, c, v) + I_{\mathrm{st}}(t), \end{aligned} \tag{16}$$

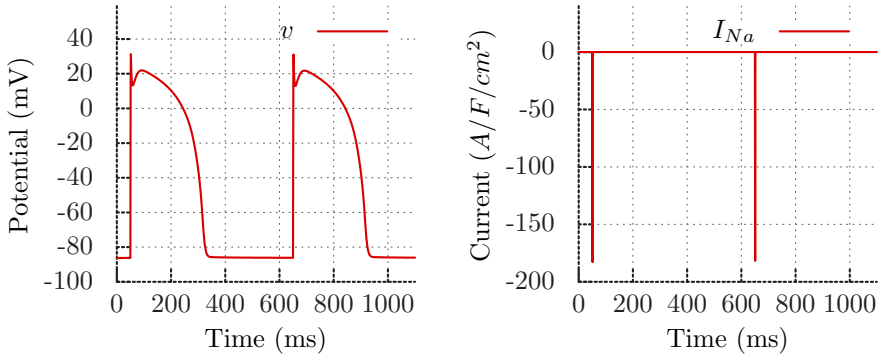

FIGURE 5. Two consecutive action potentials for the TNNP model: transmembrane potential v (left) and the fast sodium current I_{Na} (right), that is the main component of I_{ion} during the fast upstroke of the action potential.

where $w = (w_1, \ldots, w_p) \in \mathbb{R}^p$ is the vector of the gating variables, $c \in \mathbb{R}^q$ is a vector of ionic concentrations or other state variables, and $v \in \mathbb{R}$ is the cell membrane potential. These equations model the evolution of the transmembrane potential of a single cardiac cell. The four functions $w_{\infty,i}(v)$, $\tau_i(v)$, $g(w,c,v)$ and $I_{\mathrm{ion}}(w,c,v)$ are given reaction terms. They characterize the cell model. The function $I_{\mathrm{st}}(t)$ is a source term. It represents a stimulation current.

Equations (16) intrinsically fit with problem (2) formulation, precisely with,

$$a(t,y) = \begin{pmatrix} -1/\tau(v) & 0 & 0 \\ 0 & 0 & 0 \\ 0 & 0 & 0 \end{pmatrix}, \quad b(t,y) = \begin{pmatrix} w_\infty(v)/\tau(v) \\ g(y) \\ -I_{\mathrm{ion}}(y) + I_{\mathrm{st}}(t) \end{pmatrix},$$

for $y = (w,c,v) \in \mathbb{R}^N$ $(N = p+q+1)$ and where $a(t,y)$ is block diagonal with $-1/\tau(v)$ the $p \times p$ diagonal matrix with diagonal entries $(-1/\tau_i(v))_{i=1\ldots p}$.

6.2. **Implementation and computational cost.** The I-EAB$_k$ and EAB$_k$ schemes are k-multistep explicit methods and so the computation of y_{n+1} requires the data y_{n-k}, $a_{n-k} := a(t_{n-k}, y_{n-k})$ and $b_{n-k} := b(t_{n-k}, y_{n-k})$ at the k-previous time steps, *i.e.* for $k = 0 \ldots k-1$.

EAB$_k$ practical implementation. The stabilizer α_n needs to be computed first at each time step. Then the $c_{nj} = b_{n-j} + (a_{n-j} - \alpha_n) y_{n-j}$, $j = 0 \ldots k-1$ are computed, defining the γ_{nj} in table 1.

The computation of y_{n+1} by formula (6) requires in addition the computation of the $\varphi_j(\alpha_n h)\gamma_{nj}$. This is a matrix-vector product in general.
In the present case of a diagonal stabilizer, it becomes a scalar-scalar product per row. The $\varphi_j(\alpha_n h)$ are computed on all diagonal entries of $\alpha_n h$. This computation simply necessitates to compute $\varphi_0(\alpha_n h) = \mathrm{e}^{\alpha_n h}$ (one exponential per non zero

diagonal entry) thanks to the recursion rule (5).
In general, property (5) can be used to replace the computation of the $\varphi_j(\alpha_n h)\gamma_{nj}$ for $j = 0..k$ by the computation of a single product $\varphi_k(\alpha_n h)\gamma$ for a vector γ given below. Denoting by $w_1 = a_n y_n + b_n$ and $w_{j+1} = \gamma_{nj} + \alpha_n h w_j$:

- the EAB_2 scheme reduces to,

$$y_{n+1} = y_n + h\left[w_1 + \varphi_2(\alpha_n h)w_2\right],$$

- the EAB_3 scheme itself becomes,

$$y_{n+1} = y_n + h\left[w_1 + \alpha_n h w_2/2 + \varphi_3(\alpha_n h)w_3\right],$$

- and eventually the EAB_4 scheme reads,

$$y_{n+1} = y_n + h\left[w_1 + \alpha_n h w_2/2 + \alpha_n h w_3/6 + \varphi_4(\alpha_n h)w_4\right].$$

I-EAB$_k$ practical implementation. In addition, the I-EAB_k method (3) requires a quadrature rule of sufficient order to preserve the scheme accuracy and convergence order. We used the Simpson quadrature rule for the cases $k = 2$, 3 and the three point Gaussian quadrature rule for k=4. We point out that a_n is assumed diagonal here so that the matrix exponentials below actually are scalar exponential.

The I-EAB_k method with Simpson quadrature rule reads,

$$y_{n+1} = \mathrm{e}^{\tilde{g}_1}\left(y_n + b_n h/6\right) + \left(\tilde{b}_1 + 4\,\mathrm{e}^{\delta}\,\tilde{b}_{1/2}\right) h/6,$$

where (with the notations of section 2.2) $\tilde{g}_1 = \tilde{g}_n(t_{n+1})$, $\delta = \tilde{g}1 - \tilde{g}_n(t_n + h/2)$, $\tilde{b}_1 = \tilde{b}_n(t_{n+1})$ and $\tilde{b}_{1/2} = \tilde{b}_n(t_n + h/2)$. These coefficients are given for $k = 2$ by,

$$\tilde{g}_1 = (3a_n - a_{n-1})\,h/2, \qquad \delta = (7a_n - 3a_{n-1})\,h/8,$$
$$\tilde{b}_1 = 2b_n - b_{n-1}, \qquad \tilde{b}_{1/2} = (3b_n - b_{n-1})/2,$$

and for $k = 3$ by,

$$\tilde{g}_1 = (23a_n - 16a_{n-1} + 5a_{n-2})\,h/12, \qquad \delta = (29a_n - 25a_{n-1} + 8a_{n-2})\,h/24,$$
$$\tilde{b}_1 = 3b_n - 3b_{n-1} + b_{n-2}, \qquad \tilde{b}_{1/2} = (15b_n - 10b_{n-1} + 3b_{n-2})\,/8,$$

The I-EAB_k method with the three point Gaussian quadrature rule reads,

$$y_{n+1} = \mathrm{e}^{\tilde{g}_1}\left(y_n + \frac{h}{18}\left(5\tilde{b}_l\,\mathrm{e}^{-\tilde{g}_l} + 8\tilde{b}_0\,\mathrm{e}^{-\tilde{g}_0} + 5\tilde{b}_r\,\mathrm{e}^{-\tilde{g}_r}\right)\right),$$

with $\tilde{b}_s = \tilde{b}_n(t_s)$, $\tilde{g}_s = \tilde{g}_n(t_s)$ for $s \in \{l, 0, r\}$ where $t_l = t_n + (1 - \sqrt{3/5}))h/2$, $t_0 = t_n + h/2$, $t_r = t_n + (1 + \sqrt{3/5}))h/2$ and with $\tilde{g}_1 = \tilde{g}_n(t_{n+1})$.
These parameters are linear combination of the data a_{n-i}, b_{n-i} for $i = 0\ldots, k-1$

with fixed coefficients. Formula for $k = 4$ follow. The parameters $\tilde{b}_s$ are given by:

$$\begin{aligned}
16\,\tilde{b}_0 =& 35\,b_n - 35\,b_{n-1} + 21\,b_{n-2} - 5\,b_{n-3}\\
40\,\tilde{b}_r =& (95 + 179\sqrt{15}/15)b_n - (107 + 119\sqrt{15}/5)b_{n-1}\\
&+ (69 + 79\sqrt{15}/5)b_{n-2} - (17 + 59\sqrt{15}/15)b_{n-3}
\end{aligned}$$

and $\tilde{b}_l$ is the radical conjugate of $\tilde{b}_r$ (the radical conjugate of $x + \sqrt{y}$ is $x - \sqrt{y}$). And finally, the parameters $\tilde{g}_s$ definition is:

$$\begin{aligned}
24/h\ \tilde{g}_1 =& 55\,a_n - 59\,a_{n-1} + 37\,a_{n-2} - 9\,a_{n-3},\\
384/h\ \tilde{g}_0 =& 297\,a_n - 187\,a_{n-1} + 107\,a_{n-2} - 25\,a_{n-3},\\
200/h\ \tilde{g}_r =& (797/4 + 45\sqrt{15})a_n - (2233/12 + 47\sqrt{15})a_{n-1}\\
&+ (1373/12 + 29\sqrt{15})a_{n-2} - (331/12 + 7\sqrt{15})a_{n-3},
\end{aligned}$$

and $\tilde{g}_l$ is the radical conjugate of $\tilde{g}_r$.

Computational cost. Consider an ODE system (1) whose numerical resolution cost is dominated by the computation of $(t, y) \mapsto f(t, y)$. This might be the case in general for *"large and complex models"*. For such problems explicit multistep methods are relevant since they will require one such operation per time step. In regard, explicit Runge Kutta will need several such operation. Implicit methods, associated to a non linear solver, may necessitate a lot of these operations, especially for large time steps when convergence is harder to reach.

In addition, the I-EAB$_k$ and EAB$_k$ schemes need several specific operations. In the case of a diagonal function $a(t, y)$ they have been previously described: the EAB$_k$ require one scalar exponential computation per non zero row of $a(t, y)$, the I-EAB$_k$ with Simpson rule needs twice more and the I-EAB$_3$ with 3 point Gaussian quadrature rule four times more.
Such a cost is not negligible, but is at worst of same order than computing $(t, y) \mapsto f(t, y)$ for complex models. For the TNNP model considered here, computing $(t, y) \mapsto f(t, y)$ costs 50 scalar exponentials whereas the EAB$_k$ implementation adds 7 supplementary scalar exponentials per time step.

In terms of cost per time step, the EAB$_k$ method is rather optimal. The relationship between accuracy and cost of the EAB$_k$ method has been investigated in [8]: more details are available in section 6.5.

6.3. **Convergence.** For the chosen application, no theoretical solution is available. Convergence properties are studied by computing a reference solution y_{ref} for a reference time step h_{ref} with the Runge Kutta 4 scheme. Numerical solutions y are computed to y_{ref} for coarsest time steps $h = 2^p h_{ref}$ for increasing p.
Any numerical solution y consists in successive values y_n at the time instants $t_n = nh$. On every interval (t_{3n}, t_{3n+3}) the polynomial $\overline{y}$ of degree at most 3 so

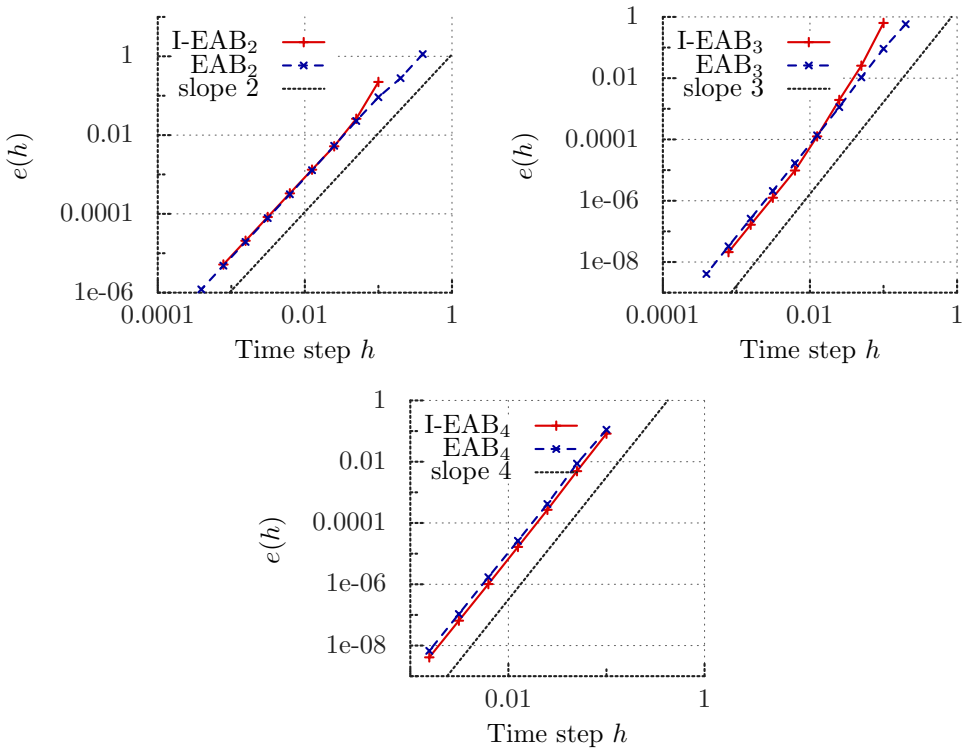

FIGURE 6. Relative L^∞ error $e(h)$ for the I-EAB$_k$ and EAB$_k$ schemes, $k = 2$, 3 and 4, and for the BR model.

that $\overline{y}(t_{3n+i}) = y_{3n+i}$, $i = 0 \dots 4$ is constructed. On $(0, T)$, $\overline{y}$ is a piecewise continuous polynomial of degree 3. Its values at the reference time instants nh_{ref} are computed. This provides a projection $P(y)$ of the numerical solution y on the reference grid. Then $P(y)$ can be compared with the reference solution y_{ref}. The numerical error is defined by,

$$e(h) = \frac{\max |v_{\text{ref}} - P(v)|}{\max |v_{\text{ref}}|}, \tag{17}$$

where the potential v is the last and stiffest component of y in eq. (16).

The numerical convergence graphs for the BR model are plotted on fig. 6. All the schemes display the expected asymptotic behavior $e(h) = O(h^k)$ as $h \to 0$, as proved in theorem 2.

6.4. **Stability.** The stiffness of the BR and TNNP models along one cellular electrical cycle (as depicted on fig. 5) has been evaluated in [27]. The largest negative real part of the eigenvalues of the Jacobian matrix during this cycle is of -1170 and -82 for the TNNP and BR models respectively. This basically means that the TNNP model is 15 times stiffer than the BR model ($15 \simeq 1170/82$).

We want to evaluate the impact of this increase of stiffness in terms of stability for the EAB_k and I-EAB_k schemes and to provide a comparison with some other classical time stepping methods. To this aim we consider the *critical time step* Δt_0. It is defined as the largest time step such that the numerical simulation runs without overflow nor non linear solver failure for $h < \Delta t_0$. The numerical evaluation of Δt_0 is quite easy for explicit methods. For implicit methods, the choice of the non linear solver certainly impacts Δt_0. Without considering more deeply this problem, we just carefully set up the non linear solver, so as to provide the largest Δt_0. In practice, we have been using a Jacobian free Krylov Newton method.

TABLE 2. Critical time step Δt_0

(a) Classical methods

	BR	TNNP
AB_2	0.124×10^{-1}	0.850×10^{-3}
BDF_2	0.306	0.158
AB_3	0.679×10^{-2}	0.464×10^{-3}
BDF_3	0.362	0.181
AB_4	0.372×10^{-2}	0.255×10^{-3}
RK_4	0.338×10^{-1}	0.255×10^{-2}
BDF_4	0.423	0.201

(b) I-EAB_k and EAB_k schemes

	BR	TNNP
I-EAB_2	0.121	0.103
EAB_2	0.424	0.233
I-EAB_3	0.103	0.123
EAB_3	0.203	0.108
I-EAB_4	0.133	0.106
EAB_4	0.122	0.756×10^{-1}

The Adams Bashforth (AB_k) and the backward differentiation (BDF_k) methods of order k have been considered, together with the RK_4 scheme.
The AB_k and the RK_4 schemes have bounded stability domain (see [11, p. 243]). Then it is expected for the critical time step to be divided by a factor close to 15 between the BR and TNNP models. Results presented in table 2 show this behavior.
The BDF_2 scheme is A-stable whereas the BDF_3 and BDF_4 are $A(\alpha)$-stable with large angle α (see [11, p. 246]). Hence the critical time step is expected to remain unchanged between the two models. Table 2 shows that the Δt_0 actually are divided by approximately 2.

The critical time steps for the I-EAB_k and EAB_k models are presented in table 2. The critical time steps for the I-EAB_k schemes remain almost unchanged from the BR to the TNNP model. For the EAB_k, they are divided by approximately 2, which behavior is similar as for the BDF_k method.

As a conclusion, for the present application, the EAB_k and I-EAB_k methods are as robust to stiffness than the implicit BDF_k schemes, though being explicit. As a matter of fact, section 5 shows that the stability domains for the I-EAB_k and EAB_k schemes depends on the discrepancy between the complete Jacobian matrix and $a(t, y)$. In the present case, $a(t, y)$ only contains a part of the Jacobian matrix diagonal. It is very interesting to notice that robustness to stiffness is actually

achieved with this choice. It is finally also interesting to see that the critical time steps of implicit and exponential methods are of the same order.

6.5. **Accuracy.** In terms of accuracy, the schemes can be compared using the relative error $e(h)$ in eq. (17).

TABLE 3. Accuracy $e(h)$ for the AB_k,I-EAB_k and EAB_k schemes: using the BR model and fixed time step $h = 10^{-3}$

	$e(h)$
AB_2	5.32×10^{-6}
I-EAB_2	8.55×10^{-6}
EAB_2	7.90×10^{-6}

	$e(h)$
AB_3	4.33×10^{-8}
I-EAB_3	4.44×10^{-8}
EAB_3	7.00×10^{-8}

	$e(h)$
AB_4	8.69×10^{-10}
I-EAB_4	7.30×10^{-10}
EAB_4	1.16×10^{-9}

The EAB_k and I-EAB_k schemes can be compared with the AB_k methods only at very small time steps, because of the lack of stability of AB_k schemes (see table 2). In table 3 are given the accuracies of these methods for a given time step $h = 10^{-3}$ and for the BR model. Ii is observed that the same level of accuracy is obtained with AB_k and EAB_k at fixed k. These figures illustrate that inside the asymptotic convergence region, EAB_k, I-EAB_k and AB_k schemes are equivalent in terms of accuracy.

TABLE 4. Accuracy for the TNNP model

	EAB_k			BDF_k		
h	$k = 2$	$k = 3$	$k = 4$	$k = 2$	$k = 3$	$k = 4$
0.1	0.351	0.530	–	–	–	0.129
0.05	9.01×10^{-2}	5.59×10^{-2}	8.93×10^{-2}	3.57×10^{-2}	1.15×10^{-2}	1.44×10^{-2}
0.025	2.14×10^{-2}	7.34×10^{-3}	8.34×10^{-3}	1.10×10^{-2}	2.58×10^{-3}	2.38×10^{-3}

Comparison at large time steps between the EAB_k and BDF_k for the TNNP model is shown in table 4. These figures show that for large time steps BDF_k is more accurate than EAB_k. A gain in accuracy of factor 2.5, 5 and 6 is observed for $h = 0.05$ and for k=2, 3 and 4 respectively. However, compare row 3 for EAB_k ($h = 0.025$) with row 2 for BDF_k ($h = 0.05$). It shows that solutions with an accuracy close to 0.01 are obtained when dividing the time step by (less than) 2 between BDF_k and EAB_k. Meanwhile, EAB_k with $h = 0.025$ costs less than BDF_k with $h = 0.05$, as developed in section 6.2. We conclude that EAB_k schemes provide a cheaper way to compute numerical solutions at large time step for a given accuracy. The same conclusion also holds for the BR model, see table 5. A deeper analysis of the relationship between accuracy and computational cost for the EAB_k scheme as compared to other methods is available in [8] with the same conclusion.

TABLE 5. Accuracy for the BR model

	EAB_k			BDF_k		
h	$k=2$	$k=3$	$k=4$	$k=2$	$k=3$	$k=4$
0.2	0.284	0.516	–	9.74×10^{-2}	4.09×10^{-2}	4.98×10^{-2}
0.1	9.26×10^{-2}	9.17×10^{-2}	0.119	3.44×10^{-2}	1.04×10^{-2}	1.27×10^{-2}
0.05	8.20×10^{-2}	1.09×10^{-2}	8.96×10^{-3}	9.74×10^{-3}	2.29×10^{-3}	2.02×10^{-3}

In table 5 are given the accuracies at large time step now considering the BR model. Comparison with table 4 shows that accuracy is preserved by dividing h by 2 when switching from the BR to the TNNP model. As already said, the TNNP model is 15 times stiffer than the BR model. We conclude that the EAB_k schemes also exhibit a large robustness to stiffness in terms of accuracy. This robustness is equivalent as for the implicit BDF_k schemes. This is quite remarkable for an explicit scheme, as for the robustness to stiffness in terms of critical time step discussed in the previous subsection.

REFERENCES

[1] W. AUZINGER AND M. LAPIŃSKA, *Convergence of rational multistep methods of adams-padé type*, tech. report, ASC Report, Vienna University of Technology, 2011.

[2] G. BEELER AND H. REUTER, *Reconstruction of the Action Potential of Ventricular Myocardial Fibres*, J. Physiol., 268 (1977), pp. 177–210.

[3] C. BÖRGERS AND A. R. NECTOW, *Exponential time differencing for Hodgkin-Huxley-like ODEs*, SIAM J. Sci. Comput., 35 (2013), pp. B623–B643.

[4] M. P. CALVO AND C. PALENCIA, *A class of explicit multistep exponential integrators for semilinear problems*, Numer. Math., 102 (2006), pp. 367–381.

[5] J. CERTAINE, *The solution of ordinary differential equations with large time constants*, in Mathematical methods for digital computers, Wiley, New York, 1960, pp. 128–132.

[6] M. T. CHU, *An automatic multistep method for solving stiff initial value problems*, J. Comput. Appl. Math., 9 (1983), pp. 229–238.

[7] S. M. COX AND P. C. MATTHEWS, *Exponential time differencing for stiff systems*, J. Comput. Phys., 176 (2002), pp. 430–455.

[8] C. DOUANLA LONTSI, Y. COUDIÈRE, AND C. PIERRE, *Efficient high order schemes for stiff odes in cardiac electrophysiology*, in African Conference on Research in Computer Science and Applied Mathematics, Tunis, 2016.

[9] S. S. DRAGOMIR, *Some Gronwall type inequalities and applications*, Nova Science Publishers, Inc., Hauppauge, NY, 2003.

[10] E. HAIRER, S. P. NØRSETT, AND G. WANNER, *Solving ordinary differential equations. I*, vol. 8 of Springer Series in Computational Mathematics, Springer-Verlag, Berlin, 1993.

[11] E. HAIRER AND G. WANNER, *Solving ordinary differential equations. II*, vol. 14 of Springer Series in Computational Mathematics, Springer-Verlag, Berlin, 2010.

[12] M. HOCHBRUCK, *A short course on exponential integrators*, in Matrix functions and matrix equations, vol. 19 of Ser. Contemp. Appl. Math. CAM, Higher Ed. Press, Beijing, 2015, pp. 28–49.

[13] M. HOCHBRUCK, C. LUBICH, AND H. SELHOFER, *Exponential integrators for large systems of differential equations*, SIAM J. Sci. Comput., 19 (1998), pp. 1552–1574 (electronic).

[14] M. Hochbruck and A. Ostermann, *Explicit Exponential Runge-Kutta Methods for Semilinear Parabolic Problems.*, SIAM J. Numerical Analysis, 43 (2005), pp. 1069–1090.
[15] M. Hochbruck and A. Ostermann, *Exponential integrators*, Acta Numer., 19 (2010), pp. 209–286.
[16] M. Hochbruck and A. Ostermann, *Exponential multistep methods of Adams-type*, BIT, 51 (2011), pp. 889–908.
[17] M. Hochbruck, A. Ostermann, and J. Schweitzer, *Exponential Rosenbrock-type methods*, SIAM J. Numer. Anal., 47 (2008/09), pp. 786–803.
[18] A. Hodgkin and A. Huxley, *A quantitative description of membrane current and its application to conduction and excitation in nerve*, J. Physiol., 117 (1952), pp. 500–544.
[19] A. Koskela and A. Ostermann, *Exponential Taylor methods: analysis and implementation*, Comput. Math. Appl., 65 (2013), pp. 487–499.
[20] D. Lee and S. Preiser, *A class of non linear multistep A-stable numerical methods for solving stiff differential equations*, Comp. & maths with appls., 4 (1978), pp. 43–51.
[21] V. T. Luan and A. Ostermann, *Explicit exponential runge kutta methods of high order for parabolic problems*, J. Comput. Appl. Math., 256 (2014), pp. 168–179.
[22] C. Luo and Y. Rudy, *A Dynamic Model of the Cardiac Ventricular Action Potential I. Simulations of Ionic Currents and Concentration Changes*, Circ. Res., 74 (1994), pp. 1071–1096.
[23] B. Minchev and W. M. Wright, *A review of exponential integrators for first order semilinear problems*, tech. report, Norwegian universtity of science and technology trondhem, 2005.
[24] S. P. Nørsett, *An A-stable modification of the Adams-Bashforth methods*, in Conf. on Numerical Solution of Differential Equations (Dundee, 1969), Springer, Berlin, 1969, pp. 214–219.
[25] A. Ostermann, M. Thalhammer, and W. M. Wright, *A class of explicit exponential general linear methods*, BIT, 46 (2006), pp. 409–431.
[26] M. Perego and A. Veneziani, *An efficent generalization of the Rush-Larsen method for solving electro-physiology membrane equations*, ETNA, 35 (2009), pp. 234–256.
[27] R. J. Spiteri and C. D. Ryan, *Stiffness Analysis of Cardiac Electrophysiological Models*, Annals of Biomedical Engineering, 38 (2010), pp. 3592–3604.
[28] K. Ten Tusscher, D. Noble, P. Noble, and A. Panfilov, *A Model for Human Ventricular Tissue*, Am J Physiol Heart Circ Physiol, 286 (2004).
[29] M. Tokman, *Efficient integration of large stiff systems of ODEs with exponential propagation iterative (EPI) methods*, J. Comput. Phys., 213 (2006), pp. 748–776.
[30] M. Tokman, J. Loffeld, and P. Tranquilli, *New adaptive exponential propagation iterative methods of Runge-Kutta type*, SIAM J. Sci. Comput., 34 (2012), pp. A2650–A2669.

Yves Coudière, INRIA Bordeaux Sud Ouest, Université de Bordeaux
E-mail address: yves.coudiere@inria.fr

Charlie Douanla Lontsi, INRIA Bordeaux Sud Ouest, Université de Bordeaux
E-mail address: charlie.douanla-lontsi@inria.fr

Charles Pierre, CNRS, LMAP, Université de Pau
E-mail address: charles.pierre@univ-pau.fr